AD-A189 327 DEVELOPMENT OF HIGH STABILITY FIBER OPTIC SPECTROPHOTOMETRIC SYSTEMS FOR..(U) PENNSYLVANIA STATE UNIV UNIVERSITY PARK DEPT OF ASTRONOMY L W RAMSEY 1/1

UNCLASSIFIED 17 FEB 87 AFGL-TR-87-0218 F19628-83-K-0038 F/G 3/1 NL

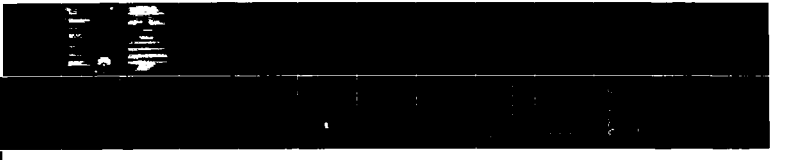

END
DATE FILMED
1-88

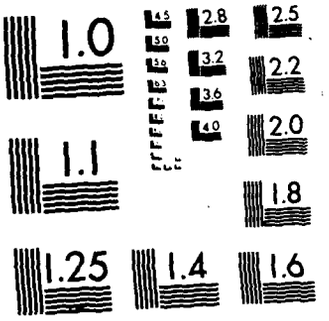

[redacted]

[redacted]

[redacted]

APPROVED FOR PUBLIC RELEASE;
DISTRIBUTION UNLIMITED

[redacted]

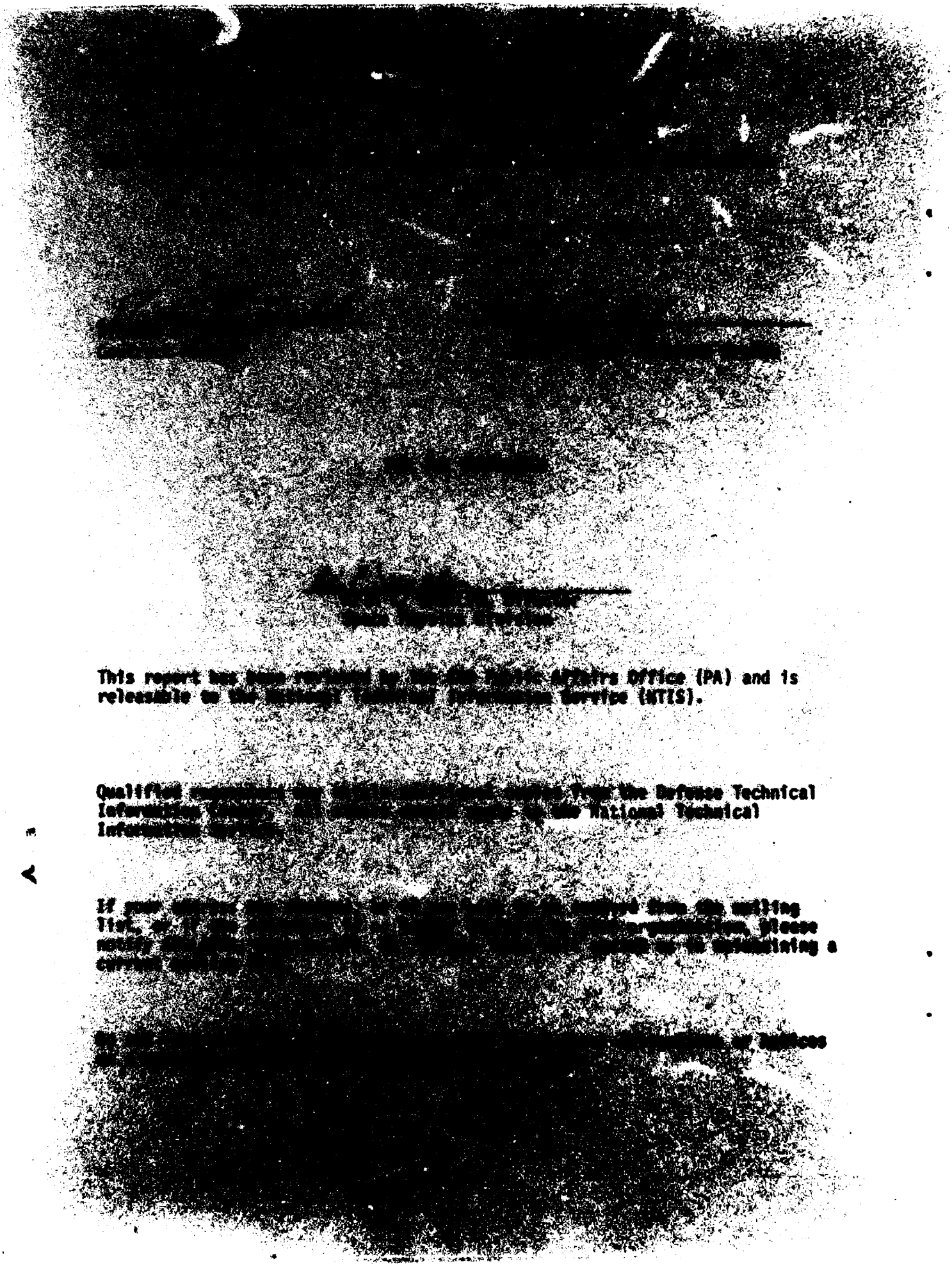

This report has been reviewed by the Public Affairs Office (PA) and is releasable to the National Technical Information Service (NTIS).

Qualified requesters may obtain additional copies from the Defense Technical Information Center. All others should apply to the National Technical Information Service.

If your address has changed, if you wish to be removed from our mailing list, or if the addressee is no longer employed by your organization, please notify [illegible] to help us maintain a current mailing list.

Do not return this copy. Retain or destroy.

Unclassified

SECURITY CLASSIFICATION OF THIS PAGE

REPORT DOCUMENTATION PAGE

1a. REPORT SECURITY CLASSIFICATION: Unclassified	1b. RESTRICTIVE MARKINGS
2a. SECURITY CLASSIFICATION AUTHORITY	3. DISTRIBUTION/AVAILABILITY OF REPORT: approved for public release; distribution unlimited
2b. DECLASSIFICATION/DOWNGRADING SCHEDULE	
4. PERFORMING ORGANIZATION REPORT NUMBER(S)	5. MONITORING ORGANIZATION REPORT NUMBER(S): AFGL-TR-87-0218
6a. NAME OF PERFORMING ORGANIZATION: Pennsylvania State University; 6b. OFFICE SYMBOL (If applicable)	7a. NAME OF MONITORING ORGANIZATION: Air Force Geophysics Laboratory
6c. ADDRESS (City, State and ZIP Code): Department of Astronomy, 525 Davey Laboratory, University Park, PA 16802	7b. ADDRESS (City, State and ZIP Code): Hanscom AFB, Massachusetts 10731
8a. NAME OF FUNDING/SPONSORING ORGANIZATION; 8b. OFFICE SYMBOL (If applicable)	9. PROCUREMENT INSTRUMENT IDENTIFICATION NUMBER: F19628-83-K-0038
8c. ADDRESS (City, State and ZIP Code)	10. SOURCE OF FUNDING NOS.

PROGRAM ELEMENT NO.	PROJECT NO	TASK NO.	WORK UNIT NO
61102F	2311	G3	CS

11. TITLE (Include Security Classification): Development of High Stability Fiber Optic Spectrophotometric Systems for Study of Solar/Stellar Magnetic Activity

12. PERSONAL AUTHOR(S): Lawrence W. Ramsey

13a. TYPE OF REPORT	13b. TIME COVERED	14. DATE OF REPORT (Yr., Mo., Day)	15. PAGE COUNT
FINAL REPORT	FROM 6/15/83 TO 6/15/86	February 17, 1987	26

16. SUPPLEMENTARY NOTATION

17 COSATI CODES			18. SUBJECT TERMS (Continue on reverse if necessary and identify by block number)
FIELD	GROUP	SUB. GR	Spectro Photometry, Fiber Optics, Solar-Stellar Activity

19. ABSTRACT (Continue on reverse if necessary and identify by block number)

We are proposing an observational program to study magnetic activity cycles in solar-type stars, including the Sun. The goal of this work is to establish the relationships between a star's magnetic-cycle morphology (i.e. amplitude, period, shape, regularity, etc.) and its age, rotation rate, and if possible, differential rotation rate, for a variety of solar-like stars. We expect to provide thereby basic empirical input into the construction of a viable dynamical dynamo theory for the Sun and the stars, leading to a deeper understanding of the ultimate origins of solar and stellar magnetism. Only when a realistic theory of magnetic field generation is available can we hope to understand fully the physics of magnetic activity, which manifests itself on all temporal and spatial scales, from transients such as flares to long-lived structures such as quiescent prominences, from flux-tubes at the limit of resolution to complex groups of sunspots. This type of program will provide fundamental support to a wide range of ongoing USAF programs studying solar magnetic activity and its impact on the solar-interplanetary and the solar-terrestrial environment. (continued)

20. DISTRIBUTION/AVAILABILITY OF ABSTRACT: UNCLASSIFIED/UNLIMITED ☐ SAME AS RPT ☐ DTIC USERS ☐	21. ABSTRACT SECURITY CLASSIFICATION: Unclassified
22a. NAME OF RESPONSIBLE INDIVIDUAL: Richard Radick	22b. TELEPHONE NUMBER (Include Area Code); 22c. OFFICE SYMBOL: AFGL/PHS

DD FORM 1473, 83 APR EDITION OF 1 JAN 73 IS OBSOLETE.

Unclassified

SECURITY CLASSIFICATION OF THIS PAGE

A critical first step in this effort was the development of an appropriate instrument. In what follows we describe an advanced-design, special-purpose, fiber fed spectrograph carefully optimized to make the required observations with maximum efficiency. In the period covered by this contract we have designed and fabricated a breadborad instrument, and tested it both in the laboratory and with telescopic observations. The results of those tests and ancillary tests of the properties of optical fibers are discussed.

1.0 Introduction

1.1 Statement of Objectives

The Primary Objective of the research conducted under this contract was to develop a very stable spectrograph system to monitor solar-like magnetic activity cycles in stars which are very close in their physical parameters to the sun. It is anticipated that the study of such stars and their activity will ultimately lead to increased understanding of the basic mechanisms of solar magnetic activity.

The time scale of the solar magnetic activity cycle is on the order of ten years and clearly if we are looking for like phenomena on other stars we will have to conduct our observation over a similar time scale. As the anticipated activity is small compared to the total output of the stars we will need high precision data. The requirement of high precision observations over a long time base will require the development of highly stable instrumentation. The research reported on here describes a design approach to such instrumentation.

1.2 Description of Approach

The approach to the problem stated above was to conduct a design study of a spectrograph and detector systems which meet the dual requirements of high precision as well as both short term and long term stability. Secondly, we constructed a functional breadboard of the system and conducted trial observations of some stars. For reasons which will become clear below, we adopted the use of optical fibers to couple the spectrograph to the telescope and this represents the key underlying approach to the problem.

The utility of step index, multimode, fused silica core fibers has been increasingly exploited in coupling telescopes to instrumentation for a variety of purposes. Hill et al. (1983) give a brief history of fiber optics in astronomical spectroscopy. The spectroscopic applications have been in two general categories. The first of these has been in multiple object spectroscopy as described by Hill et al. (1982), Gray (1983), and Tubbs et al. (1982).

Secondly, fibers have been used to couple existing spectrographs to telescopes as pioneered by Hubbard et al. (1979) and Heacox (1980). More recently many other groups have done this. Examples in the literature include Schiffer (1983), and Enard and Lund (1983). For our purposes here, we have specifically developed a spectrograph optimized for fiber optic coupling to a telescope at cassegrain focus.

The advantages of feeding a spectrograph are several. Most important is the high illumination stability afforded by the image scrambling capability of the fiber. Seeing and guiding fluctuations at the input are largely converted to intensity variations over the entire pupil in the spectrograph. This leads to superior flat field performance, which is extremely important in doing very high signal-to-noise (S/N) spectroscopy with CCD's. It also provides excellent radial velocity stability since the zonal errors enumerated by Tull (1972) are largely eliminated. Removing the instrument from the back of the telescope eliminates flexure problems which are also an important factor in the cost of a cassegrain instrument. A spectrograph built on an optical bench is economical, versatile and mechanically stable. Finally, the ability to feed an instrument in a controlled environment enhances the system stability and reliability. A substantial advantage for the study of solar/stellar magnetic activity is that once the instrument is developed it can be used on a variety of telescopes and can be expected to give the same performance. There are two disadvantages of fiber coupling; poor violet transmission and input focal ratio degradation.

2.0 Research Accomplishments

2.1 Fiber Optics

As an initial step we evaluated a variety of step index multimode fibers available on the market. Transmission is usually characterized by the manufacturer. Figures 1 thru 4 show the transmissions of several fibers we

measured in our lab. They include end reflection losses from a polished fiber. Losses in approximately 15 meters of fiber, such as we use, are comparable to a "real" aluminum mirror in the blue, i.e., less in the red and more in the violet short of 380 nm. Figure 3 illustrates the transmission of a "dry" fiber, which is much poorer in the blue. It lacks the hydroxyl absorption around 700 and 900 nm. This fiber has some advantages in the far red but was rejected for the instrument considered here as we wanted good transmission near the Ca II K line (λ = 393 nm).

The focal ratio degradation (FRD) is almost never addressed in a useful form by manufacturers and should always be measured since it is sensitive to both the manufacturing and packaging process. Barden et al. (1981), Gray (1983) and Powell (1983) have presented measurements and have discussed its causes. Figure 5 illustrates measurements we made which illustrate how the fiber can lower throughput by increasing the speed of the output beam relative to the input beam. This FRD effect is the most important difficulty encountered in using fibers to couple telescopes to spectrographs. The effect of the FRD can be minimized by designing an instrument specifically for use with a fiber coupler as we have done here.

2.2 Spectrograph Design

The scientific motivation for this instrument was to obtain moderate resolution spectra of stars with high signal-to-noise and radial velocity stability. It was deemed particularly desirable to obtain as near complete spectral coverage as possible. This is best achieved with an echelle format on a CCD. The requirement of obtaining spectra at the Ca II K line at 394 nm simultaneously with spectra at 855 nm led to a design with two beams feeding separate gratings and collimators. A fundamental constraint on the design was imposed by the fiber itself. We prefered to directly illuminate the collimator with the fiber in order to keep the efficiency high. At the same time we wanted to keep

the collimator as slow as possible so we could obtain good matching of a resolution element on the CCD without excessively fast optics. Our experience indicated that working at about f/6 was the best choice as very little light is lost (see Figure 5) when the fiber is illuminated at f/8.

A computer modeling program, using the equations for echelle grating geometry, was developed to explore various spectrograph geometries. These equations are described by Schroeder and Hillard (1980). Our program did not treat in any detail the optical aberrations of the various elements. With a target spot size of about 60 microns, to match the 30 micron CCD pixels, initial estimates indicated that likely aberrations were ignorable.

Figure 6 details the configuration we adopted in our final design. The spectrograph has two beams as mentioned above which are split off the single fiber by a beamsplitter. We effectively have two spectrographs which we refer to as the "red" and the "blue" spectrographs. Each has a f/6 collimator which is well matched to the effective fiber output f-ratio. An echelle grating, which is a 79 line R = 2 ruling 100 mm x 200 mm, is used in the red spectrograph. The grating is slightly overfilled and is the effective system aperature stop. This overfilling represents approximately a 10% loss.

Figure 6 shows the red spectrograph is in a Quasi-Littrow (QL) configuration. Schroeder and Hillard (1980) have shown that the highest peak efficiencies across an order are obtained using this configuration. The lack of any anamorphic magnification in this configuration aids one in taking advantage of commercially available camera lenses. In the QL geometry, the angle of incidence is equal to the diffraction angle, but the dispersed beam from the echelle is directed back above the collimated input beam at an angle gamma, here 20 degrees, toward a cross dispersing prism. This prism is a 60 degree prism of F2 glass. This cross dispersing prism is illuminated at minimum deviation. A prism is much more desirable as a cross dispersing element since its dispersion increases towards

shorter wavelengths where the free spectral range of the echelle is becoming smaller, thus allowing a more optimal packing of the spectra on the CCD. In addition, the major losses are fresnel surface reflection losses which are relatively small in the red. A Nikon 200 mm f/2 camera lens yields excellent images on a CCD from 450 nm to over 900 nm with only a little achromatism apparent at the red end. Table 1 shows the orders present and the cross dispersed order positions. A CCD with 512 x 512, 0.03 mm pixels is assumed.

Table 1

Grating = 79.0 Lines/MM — Blaze Angle = 63.43 Deg.
Camera Focal Length = 200.0 MM — Fiber Core Dia = .2000
Collimator Focal Length = 600.00 MM
Theta = .00 Gamma = 10.00 — Grating tilt = -.200
Anamorphic Magnification = 1.0000

ORDER	LAMCENTR	FSR	LOWLAM	HILAM	DISP (A/MM)	RES: (A)	PIX
23	9678.13	420.79	9584.38	9771.87	12.21	.81	2.22
24	9274.87	386.45	9185.03	9364.71	11.70	.78	2.22
25	8903.88	356.16	8817.63	8990.12	11.23	.75	2.22
26	8561.42	329.29	8478.49	8644.35	10.80	.72	2.22
27	8244.33	305.35	8164.48	8324.18	10.40	.69	2.22
28	7949.89	283.92	7872.89	8026.89	10.03	.67	2.22
29	7675.76	264.68	7601.41	7750.10	9.68	.65	2.22
30	7419.90	247.33	7348.03	7491.77	9.36	.62	2.22
31	7180.55	231.63	7111.00	7250.10	9.06	.60	2.22
32	6956.15	217.38	6888.78	7023.53	8.77	.58	2.22
33	6745.36	204.40	6680.03	6810.70	8.51	.57	2.22
34	6546.97	192.56	6483.55	6610.38	8.26	.55	2.22
35	6359.91	181.71	6298.31	6421.51	8.02	.53	2.22
36	6183.25	171.76	6123.36	6243.14	7.80	.52	2.22
37	6016.13	162.60	5957.86	6074.40	7.59	.51	2.22
38	5857.81	154.15	5801.07	5914.55	7.39	.49	2.22
39	5707.61	146.35	5652.33	5762.90	7.20	.48	2.22
40	5564.92	139.12	5511.02	5618.82	7.02	.47	2.22
41	5429.19	132.42	5376.61	5481.78	6.85	.46	2.22
42	5299.93	126.19	5248.59	5351.26	6.68	.45	2.22
43	5176.67	120.39	5126.53	5226.81	6.53	.44	2.22

Crossdispersed positions in millimaters for above

PRISM APEX = 60.0000 Degrees — Incident Angle - 53.8000
Glass is F2 — Minimum deviation Angle = 53.8018 Deg.

ORDER	DELTA Y POSITIONS			REF. ANGLE	DEL Y
23	8.227	8.296	8.364	52.8255	.0000
24	7.914	7.987	8.059	52.9141	.3093
25	7.596	7.674	7.749	53.0039	.3134
26	7.273	7.355	7.435	53.0952	.3187
27	6.942	7.029	7.114	53.1884	.3254
28	6.604	6.696	6.787	53.2839	.3332

29	6.256	6.354	6.450	53.3819	.3420
30	5.898	6.003	6.105	53.4826	.3517
31	5.529	5.641	5.749	53.5863	.3620
32	5.148	5.267	5.383	53.6932	.3733
33	4.755	4.882	5.006	53.8035	.3850
34	4.350	4.485	4.616	53.9175	.3977
35	3.930	4.074	4.213	54.0352	.4109
36	3.496	3.649	3.797	54.1568	.4246
37	3.047	3.210	3.368	54.2827	.4393
38	2.583	2.756	2.923	54.4128	.4543
39	2.102	2.285	2.463	54.5475	.4701
40	1.604	1.799	1.988	54.6869	.4866
41	1.088	1.295	1.495	54.8312	.5038
42	.554	.773	.986	54.9807	.5216
43	.000	.233	.458	55.1355	.5403

CROSS DISPERSED DEMAGNIFICATION = .9746

In this design the optical demagnification is such that a spectral resolution element subtends 2.2 pixels on the CCD. The QL geometry has not been used often in slit spectrographs because it introduces a rotation of the slit image which is a function of the gamma angle. This can add considerable difficulty to the data reduction process as well as ultimately degrade the realizable resolution. This was of little consequence since the fiber "slit" is circular.

The blue spectrograph is rather conventional using a 1200 line grating in the 3rd order where the region of interest, 389-405 nm, is near the blaze. A special optimized blue camera is required. Table 2 shows the parameters for this beam.

Table 2

Grating = 1200.0 Lines/MM — Blaze Angle = 46.07 Deg.
Camera Focal Length = 400.0 MM — Fiber Core Dia = .2000
Collimator Focal Length = 900.00 MM
Theta = 6.00 — Gamma = .00 — Grating Tilt = .000
Anamorphic Magnification = 1.2449

ORDER	LAMCENTR	FSR	LOWLAM	HILAM	DISP (A/MM)	RES: (A)	PIX
2	5968.29	2984.14	5907.06	6029.51	7.97	.57	2.38
3	3978.86	1326.29	3938.04	4019.67	5.31	.38	2.38

2.3 The CCD Detactor System

A CCD detector is best suited for the high S/N type of data required by the ultimate scientific goals. We developed a CCD system for the red spectrograph breadboard discussed below. Our CCD detector system is straightforward and

consists mostly of commercially available hardware. Figure 7 is a functional block diagram of this system. The control software on the LSI 11/23 system was written in FORTH. An interesting feature of our system is the cache memory which accepts the data directly from the CCD camera and is read at leisure by the computer. It is currently configured 16 bits deep for a 512 x 512 array, but is trivially expandable to 2 Mb in the current chassis.

The CCD is a RCA 512 x 320 SID501 chip which performs very well. We have determined the system noise floor to be 40 electrons and the chip itself has very few cosmetic defects. The biggest problem with the RCA device is the background radiation which occurs at a rate of about 350 events per hour. Their energy distribution peaks at about 800 electrons and falls off rapidly toward higher energies. The Corning 0211 glass, on which the CCD is bonded, is the most likely source of these "spikes", as it has potassium in it. The spikes are almost always single pixel events. While this is not a problem for the high S/N work we concentrate on, it does limit the usefulness of this CCD in long exposure, low to moderate S/N work.

2.4 Breadboard spectrograph at Penn State

A completely functional and nearly optically identical instrument which mimics the performance of the red beam of the spectrograph proposed for a long term monitoring program of stellar magnetic cycles was constructed at Penn State. The construction of this instrument and the CCD detector system was partially funded by NSF as well as this contract. We used this system for over a year and have found it to meet all of our design goals.

Figure 8 illustrates a cut perpendicular to the spectral dispersion for a flat field exposure which is taken every night. A fit made to this locates the position of the individual orders on the CCD with a resulting map such as displayed in Figure 9. This order map is derived from quatrz lamp flat fields and illustrates the slight order curvature introduced by the prism cross disperser geometry. Typically we obtain useful data in 34 orders on a well exposed spectrum. The height and width of the orders is used to compute the total intensity at each point in the order for both the flat field and subject spectrum. Figure 10

illustrates a flat field order and background. The latter is mostly bias and scattered light as dark signal is negligable. Each stellar spectral order is divided by the corresponding flat field to remove fixed pattern response as well as optical system vignetting. Figure 11 shows reduced spectra for the H-alpha region of Chi 1 Ori. There are two spectra plotted on each of these figures as well as the difference between them. This difference is an excellent estimate of the signal to noise ratio. The computed rms values for these differences yield S/N = 100. As the data displayed on Figure 11 were taken on different nights the excellent comparison also illustrates the stability of the system.

Stability of the system was also studied by using the flat fields. Absolutely essential is the stability of the flat fields over at least one night. Figure 12 shows two flat fields taken about 8 hours apart and the ratio between them. The residual ripple in this ratio is indicative of a color change in the lamp of a few percent and not a shifting of the CCD or other system components. Such shifts would have a differential signature. We conclude that our flat field illumination is stable in position to a small fraction of a pixel and is adequate for S/N >> 200.

We have observed several radial velocity standards in the QL configuration and find that nightly dispersions are on the order of 1 km/sec. This is with a resolution of 12000 over 2.2 pixels. Thus the radial velocity stability is on the order of 0.1 pixel. This is a major benefit of the fiber scrambling. Ramsey and Huenemoerder (1986) discuss the results for several other trial observations of stars.

2.5 References

Barden, S.C., Ramsey, L.W., and Truax, R.J. 1981, P.A.S.P., 93, 154.

Barden, S.C., Ramsey, L.W., and Truax, R.J. 1980, BAAS, 12, 460.

Diego, F. 1985, P.A.S.P. 97, 1209.

Enard, D. and Lund G. 1983, ESO Messenger No. 31.

Gray, P.M. 1983, Proc. S.P.I.E., 445, 57.

Heacox, W. 1980, Optical and Infrared Telescopes of the 1990's, ed. A. Hewitt (Tucson: KPNO), p. 702.

Hubbard, E.N., Angel, J.R.P., and Gresham, M.S. 1979, Ap.J., 229, 1074.

Hill, J.M., Angel, J.R.P., and Scott, J.S. 1983, Proc. S.P.I.E. 380, 354.

Hill, J.M., Angel, J.R.P., Scott, J.S., Lindley, D., and Hintzen, P. 1982, Proc. S.P.I.E., 331, 279.

Powell, J.R. 1983, Proc. S.P.I.E., 445, 77.

Ramsey, L.W., Barden, S.C., Nations, H.L., and Truax, R.J. 1981, BAAS, 12, 836.

Ramsey, L.W., Huenemoerder, D.P. 1986, Proc. S.P.I.E. 627, p. 282.

Schiffer, J.G.V. 1983, Proc. S.P.I.E., 445, 52.

Schroeder, D.J. and Hillard, R.L. 1980, Applied Optics, 19, 2833.

Schroeder, D.J., "Methods of Experimental Physics, Vol. 12A", N. Carlton, Ed., (Academic, New York, 1974), pp. 463-489.

Tubbs, E.F., Goss, W.C., and Cohen, J.C. 1982, Proc. S.P.I.E., 331, 289.

Tull, R.G. 1972, in ESO/CERN Conference on Auxiliary Instrumentation for Large Telescopes, ed. S. Lausten & A. Reiz, p. 259.

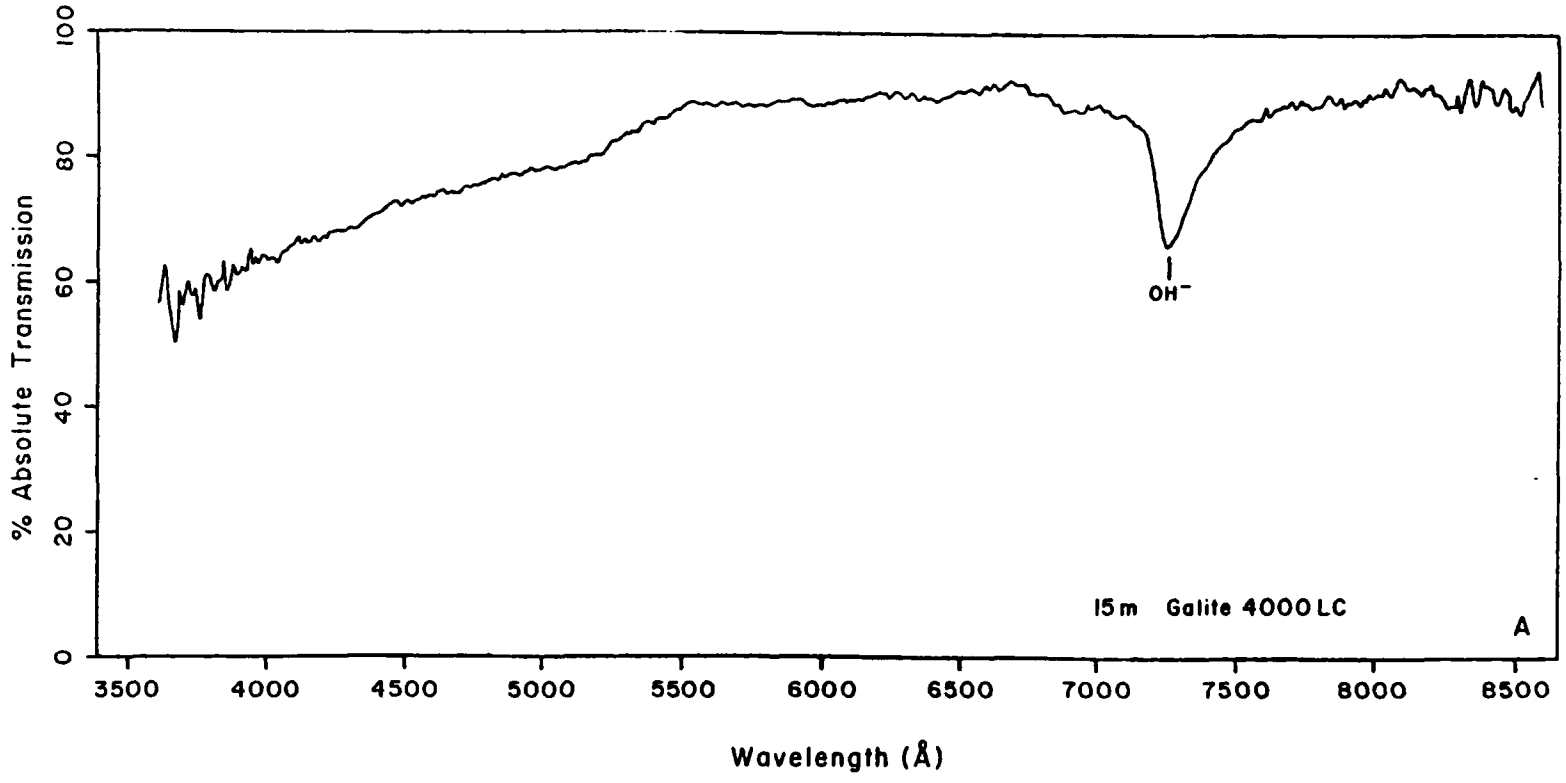

Figure 1: The absolute transmission for a 15 meter length of Galite 4000LC which is a 200 micron core plastic clad fiber. Note strong hydroxl absorption.

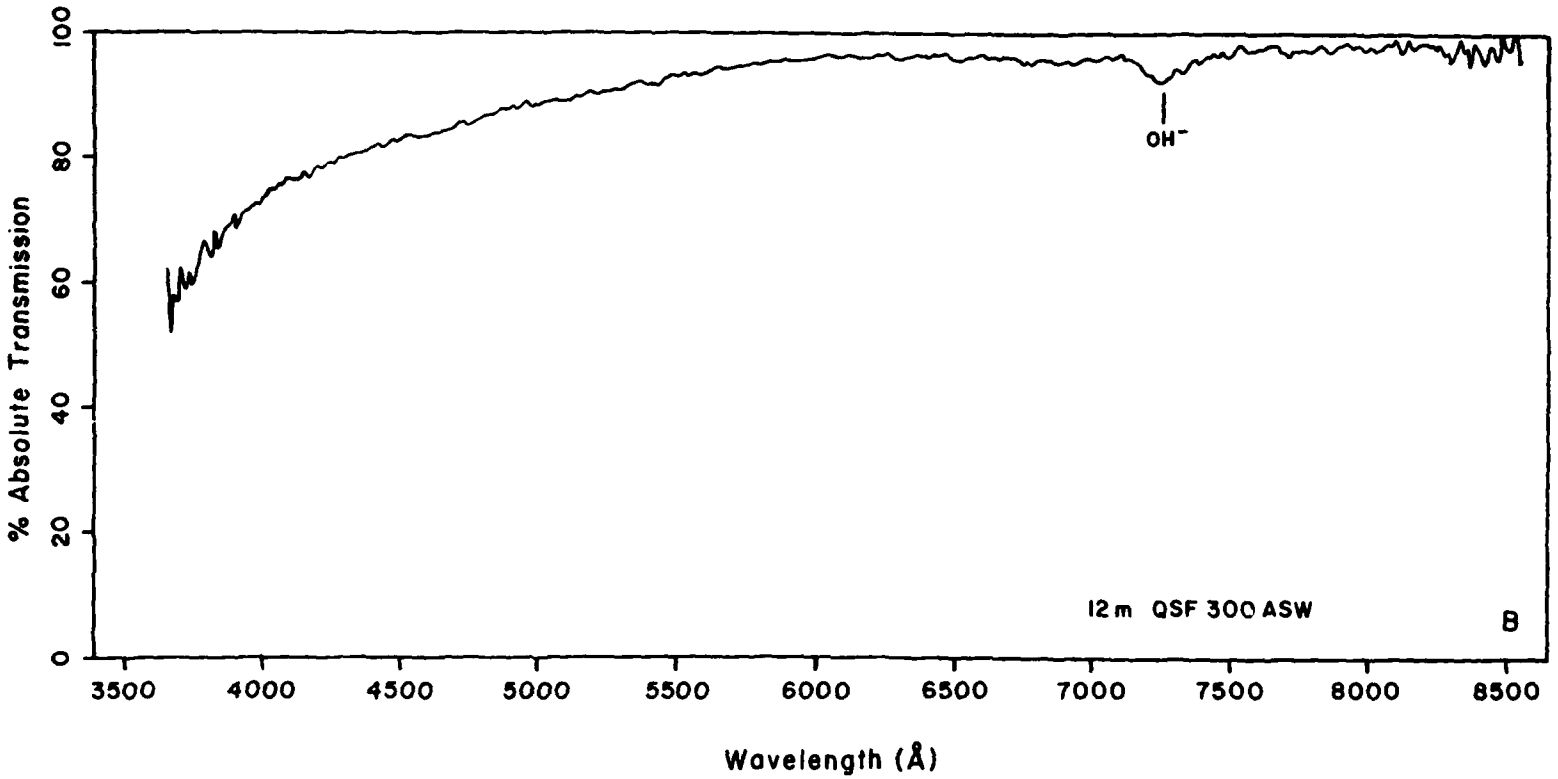

Figure 2: The absolute transmission of a 12 meter sample of QSF 300 ASW fiber is given here. This measurement includes end reflection losses. This 200 micron core fiber is glass clad. While a "wet" fiber the hydroxl absorption is less than the Galite.

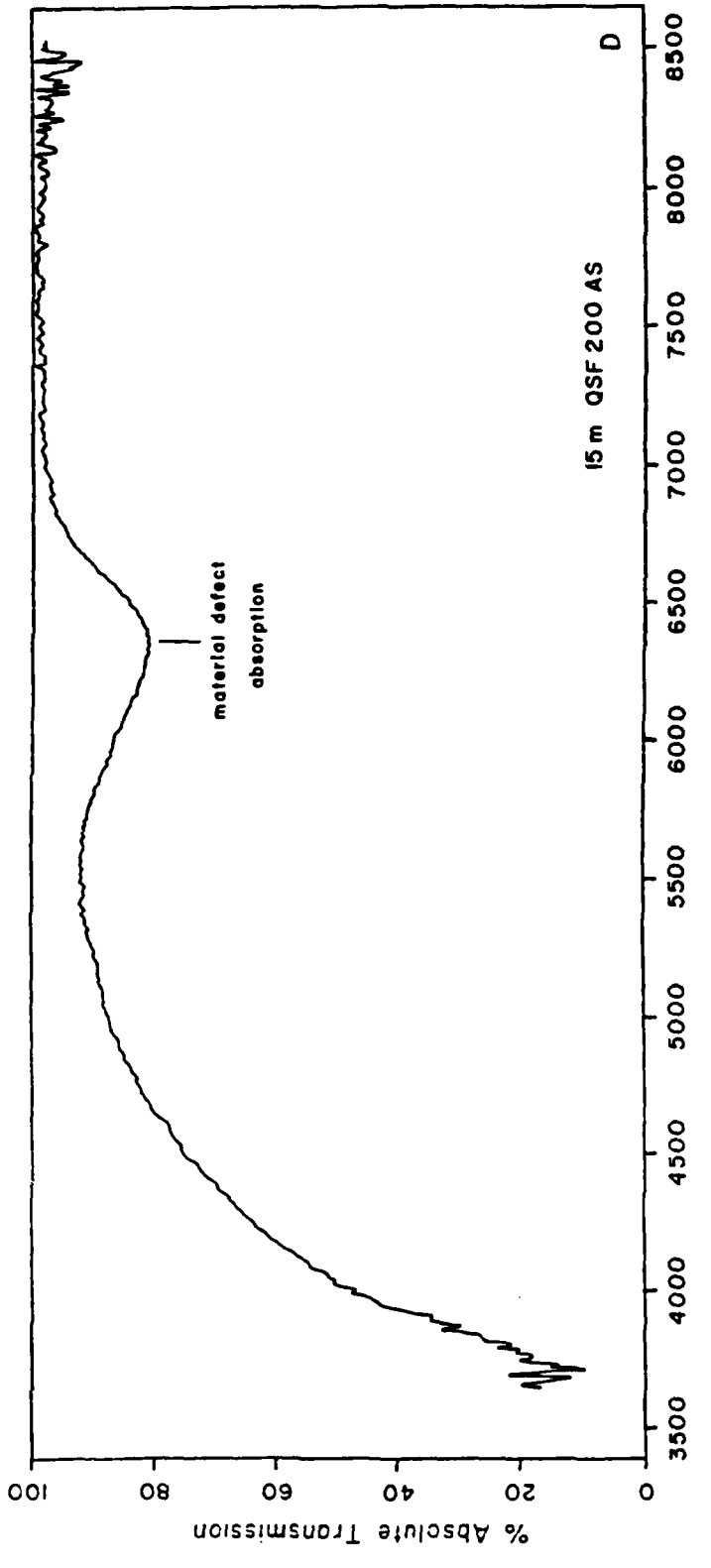

Figure 3: Absolute transmission for a QSF 200 AS fiber. This "dry" fiber also has a 200 micron core but much poorer blue transmission.

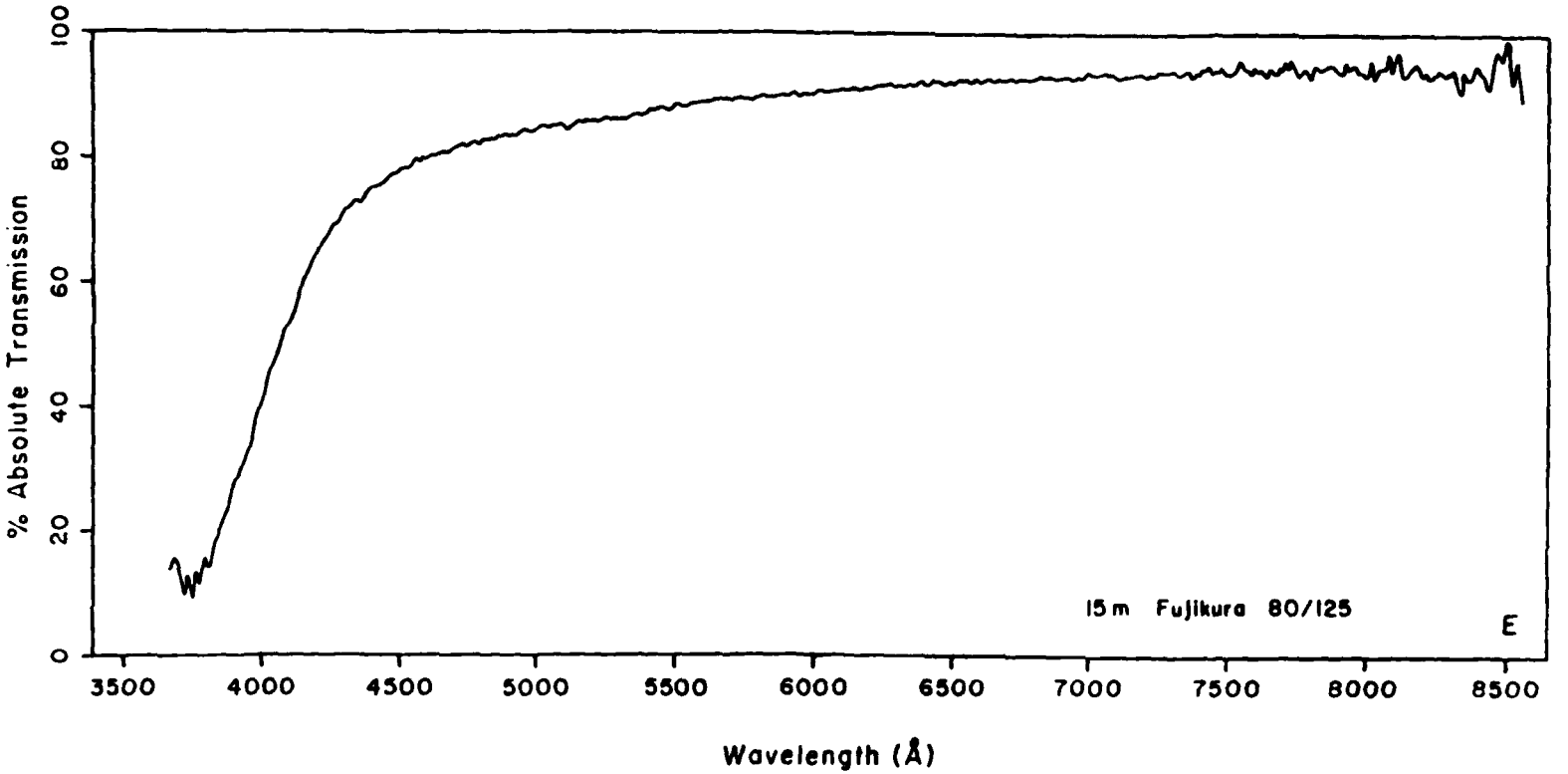

Figure 4: The Fujikuro fiber for which the transmission is displayed here has a 85 micron core. Violet transmission is poor.

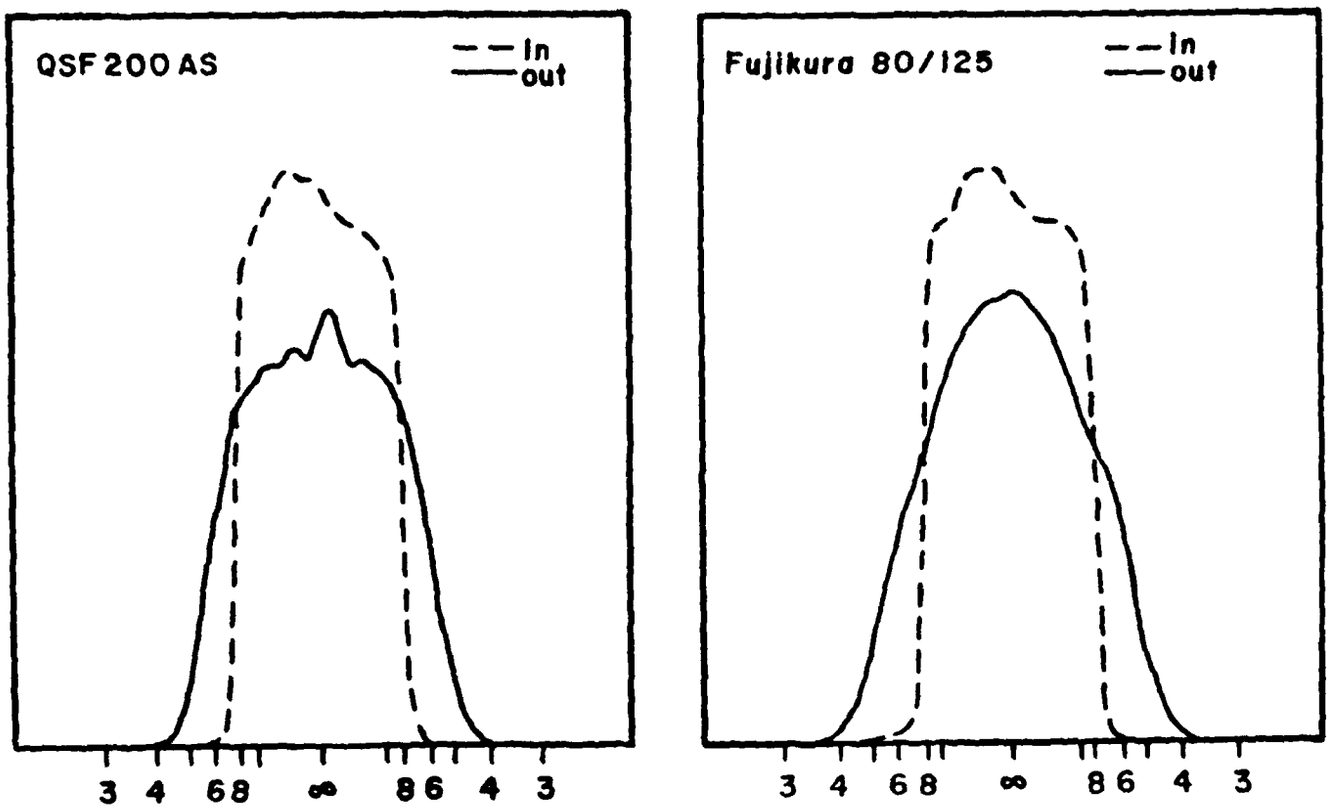

Figure 5: A measurement of the focal ratio degradation (FRD) for samples of QSF 300 AS and Fujikua fibers are illustrated here. The input beam is from a lens illuminated with collimated light and stopped down to f/8. The output profile was measured by scanning a fiber coupled to a PMT at a known distance from the sample fiber.

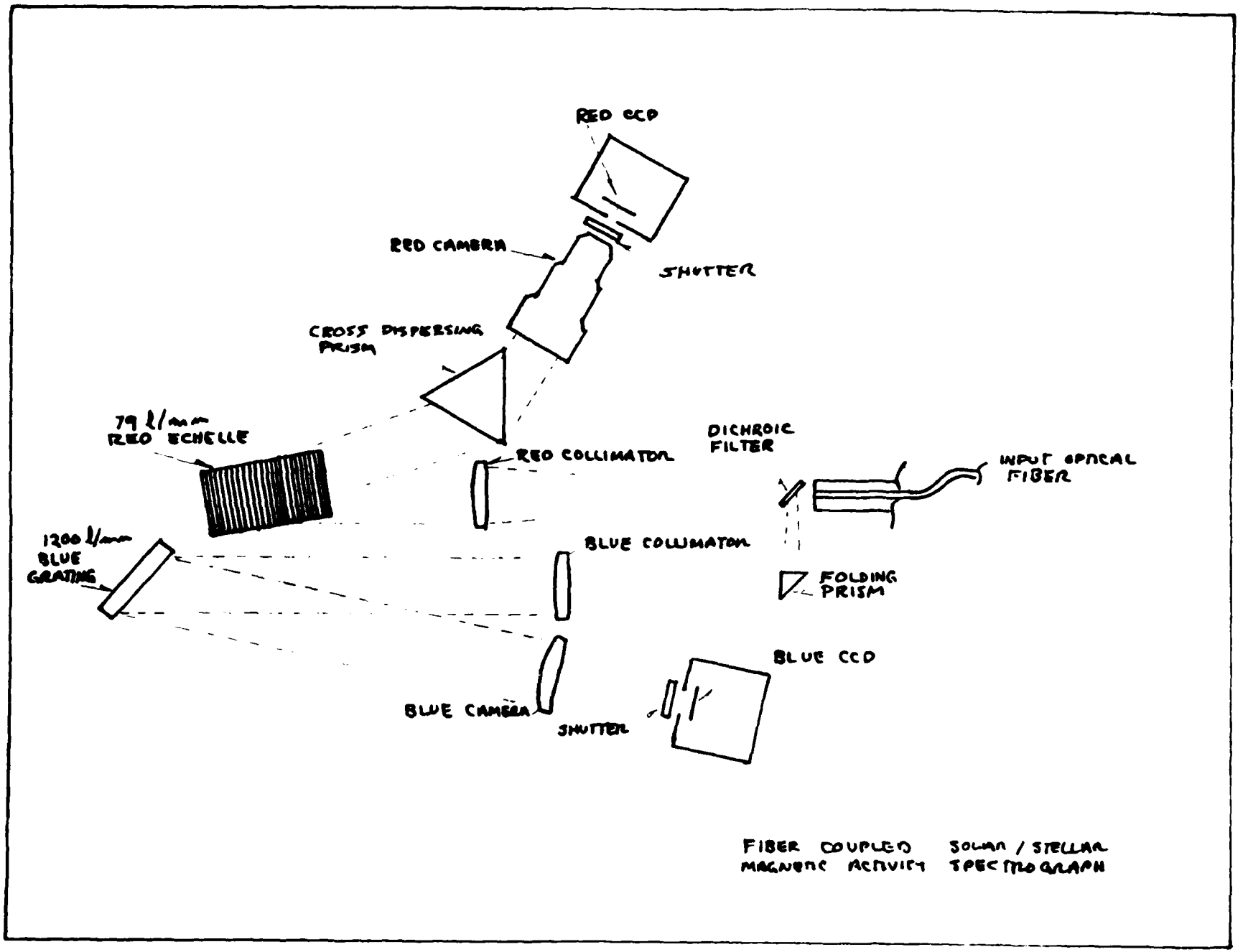

Figure 6: Illustrated here is the optical layout of the final design of the spectrograph for the magnetic cycles program.

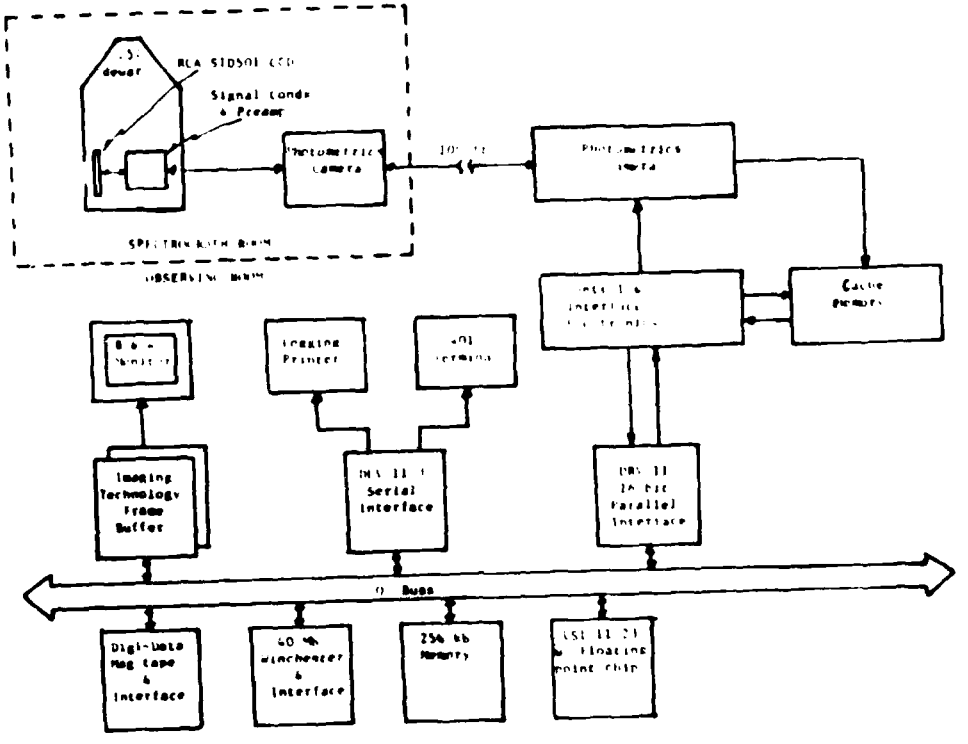

Figure 7: The above block diagram is the CCD detector and computer system that is used with the echelle spectrograph.

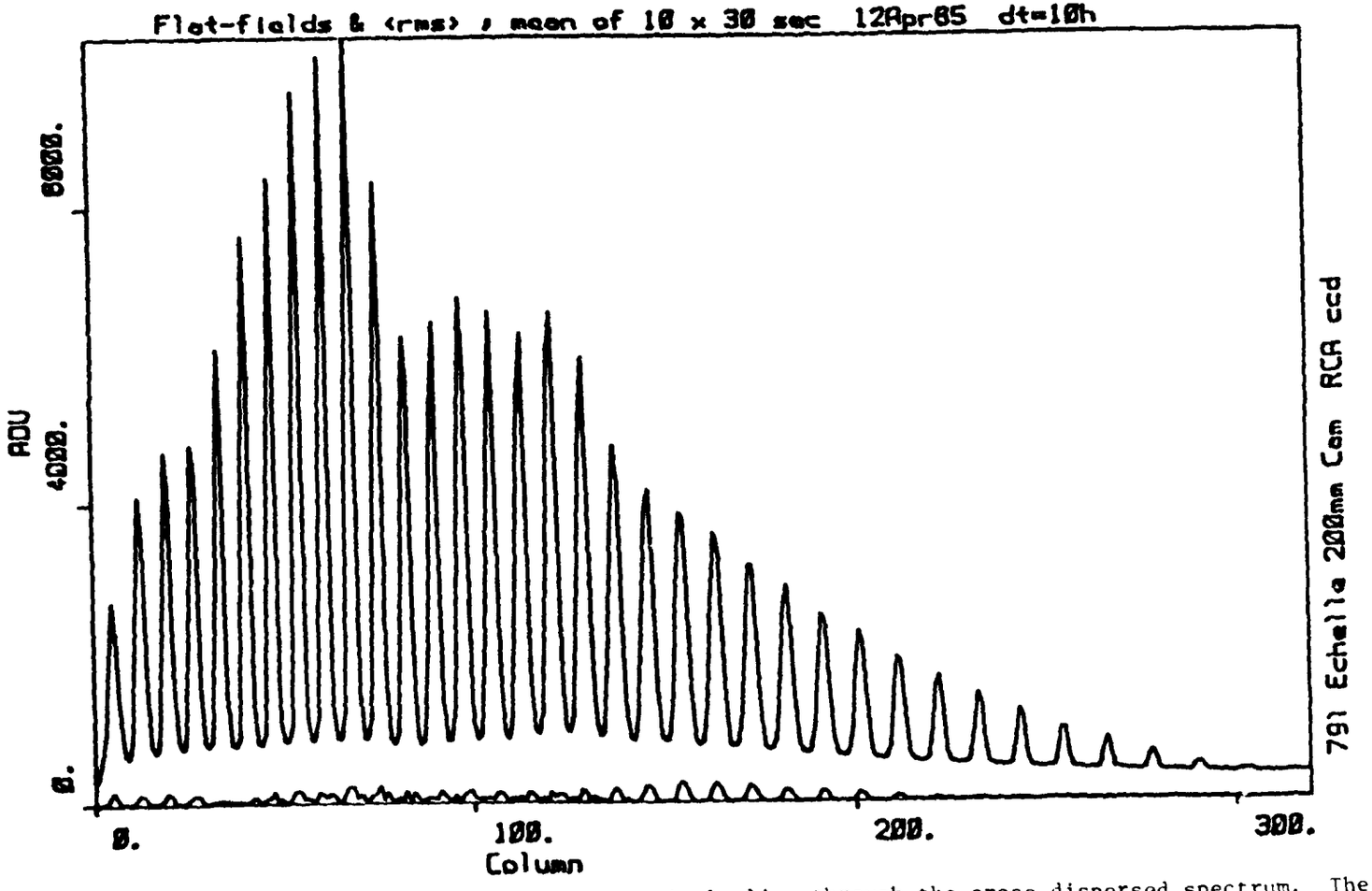

Figure 8: This cut at row 256 represents a vertical slice through the cross dispersed spectrum. The solid line represents the data and a dotted line (hardly visible) is a model fit to that data. The residual between the data and model is plotted at the bottom magnified 5 times.

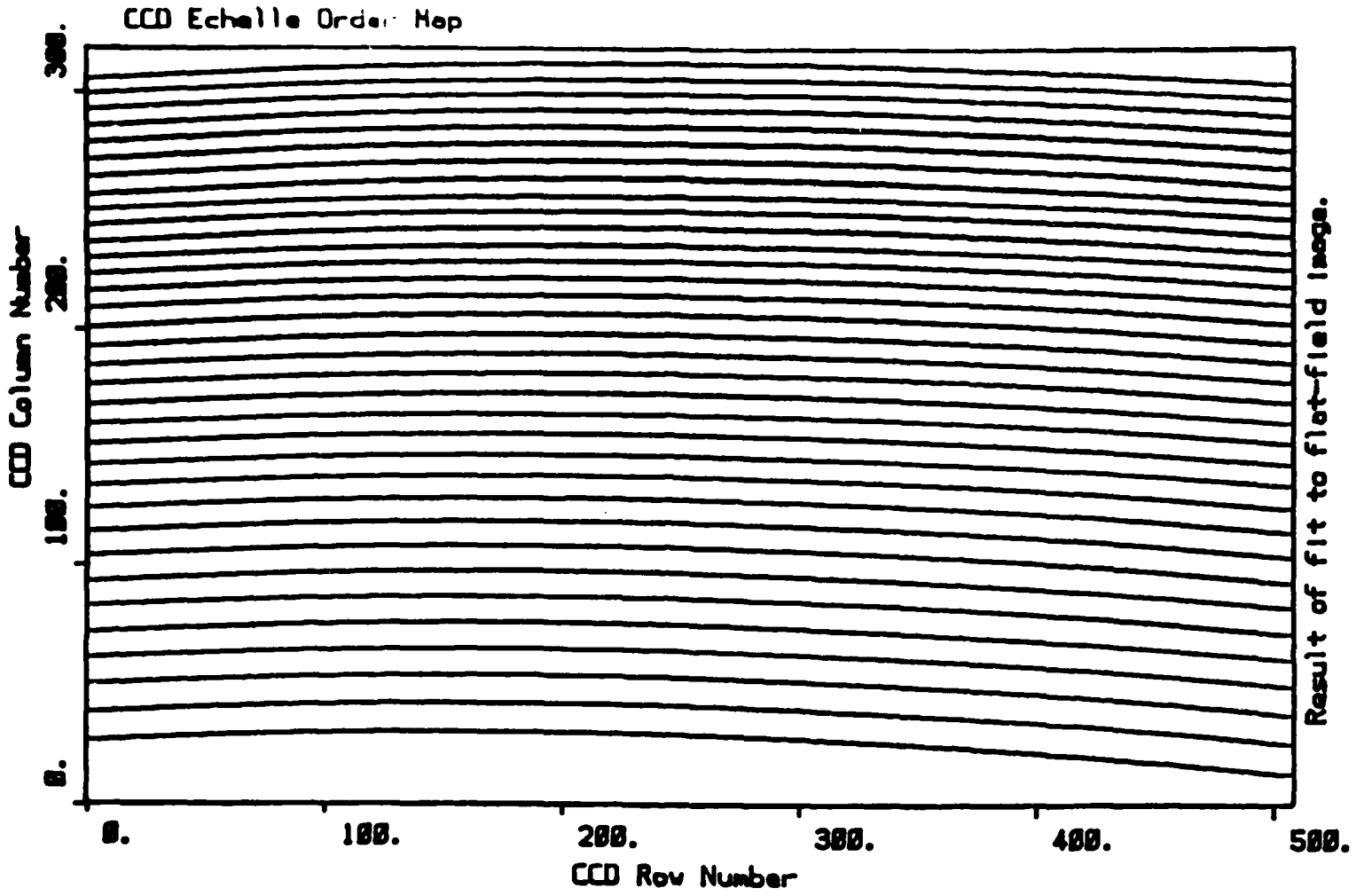

Figure 9: This order map is derived from flat field frames taken every night we observe. It is an initial step in the reduction process and shows the location of the centers of all the orders on the CCD.

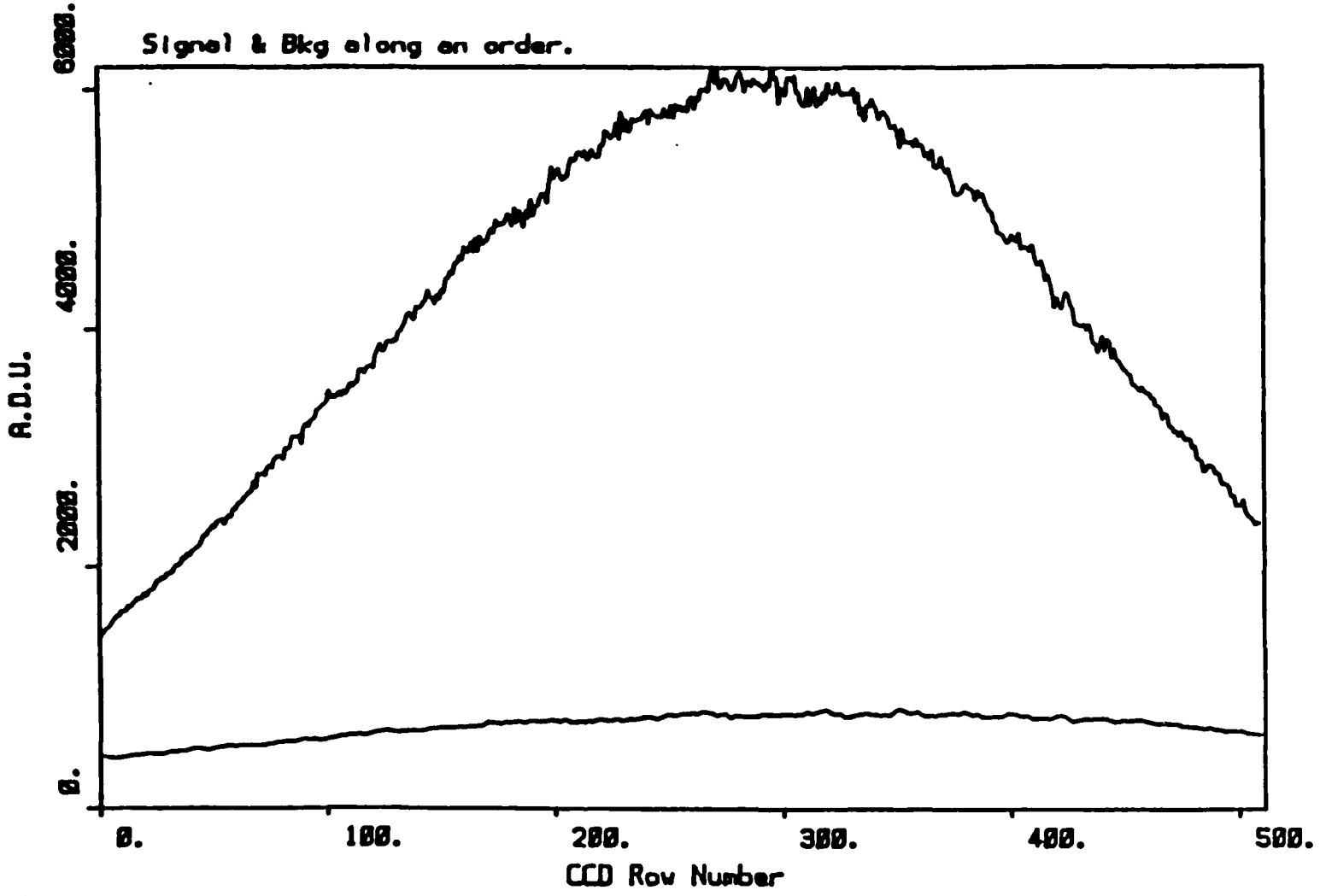

Figure 10: We show here what a single order of a flat field spectrum looks like in the direction of dispersion. The shape largely reflects the blaze function.

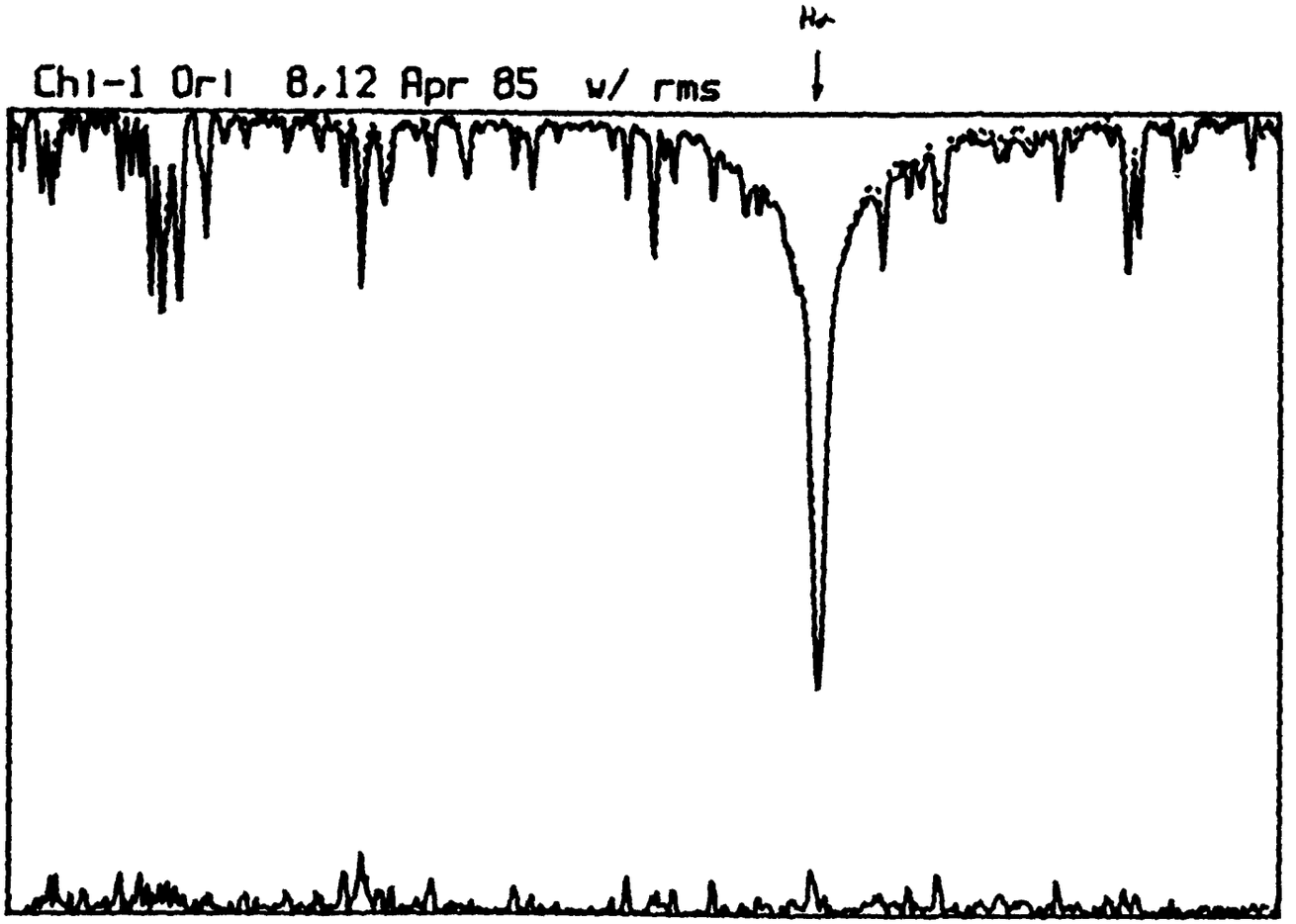

Figure 11. This figure shows sample spectra of an active solar-like star taken on different nights The RMS difference between the spectra after all reduction is about 1%. This difference is plotted at the bottom where some of the more noticable differences are due to imperfect cancellation of water vapor lines.

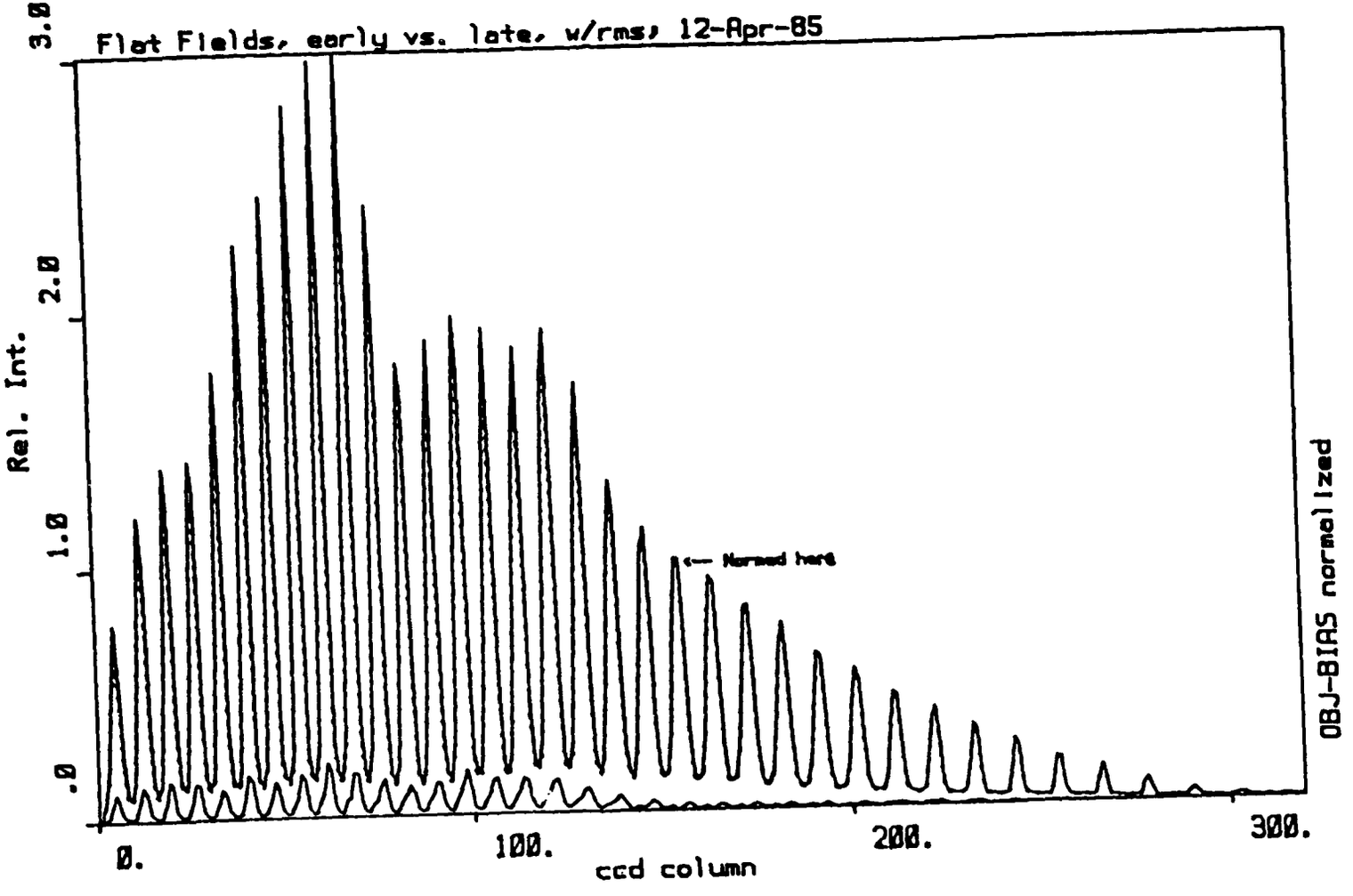

Figure 12: We here show two flat fields taken about 8 hours apart as well as the difference between them magnified by 10.

3.0 Summary of Publication Submitted

All publications resulting from this contract fully or partially are listed below.

Ramsey, L.W., Huenemoerder, D.P. 1986, Proc. S.P.I.E. 627, p. 282.


DATE
FILMED
8